

# Salvicine Inactivates $\beta_1$ Integrin and Inhibits Adhesion of MDA-MB-435 Cells to Fibronectin via Reactive Oxygen Species Signaling

Jin Zhou, Yi Chen, Jing-Yu Lang, Jin-Jian Lu, and Jian Ding

Division of Anti-tumor Pharmacology, State Key Laboratory of Drug Research, Shanghai Institute of Materia Medica, Chinese Academy of Sciences, Shanghai, People's Republic of China

## Abstract

Integrin-mediated adhesion to the extracellular matrix plays a fundamental role in tumor metastasis. Salvicine, a novel diterpenoid quinone compound identified as a nonintercalative topoisomerase II poison, possesses a broad range of antitumor and antimetastatic activity. Here, the mechanism underlying the antimetastatic capacity of salvicine was investigated by exploring the effect of salvicine on integrin-mediated cell adhesion. Salvicine inhibited the adhesion of human breast cancer MDA-MB-435 cells to fibronectin and collagen without affecting nonspecific adhesion to poly-L-lysine. The fibronectin-dependent formation of focal adhesions and actin stress fibers was also inhibited by salvicine, leading to a rounded cell morphology. Furthermore, salvicine down-regulated  $\beta_1$  integrin ligand affinity, clustering and signaling via dephosphorylation of focal adhesion kinase and paxillin. Conversely, salvicine induced extracellular signal-regulated kinase (ERK) and p38 mitogen-activated protein kinase (MAPK) phosphorylation. The effect of salvicine on  $\beta_1$  integrin function and cell adhesion was reversed by U0126 and SB203580, inhibitors of MAPK/ERK kinase 1/2 and p38 MAPK, respectively. Salvicine also induced the production of reactive oxygen species (ROS) that was reversed by ROS scavenger *N*-acetyl-L-cysteine. *N*-acetyl-L-cysteine additionally reversed the salvicine-induced activation of ERK and p38 MAPK, thereby maintaining functional  $\beta_1$  integrin activity and restoring cell adhesion and spreading. Together, this study reveals that salvicine activates ERK and p38 MAPK by triggering the generation of ROS, which in turn inhibits  $\beta_1$  integrin ligand affinity. These findings contribute to a better

understanding of the antimetastatic activity of salvicine and shed new light on the complex roles of ROS and downstream signaling molecules, particularly p38 MAPK, in the regulation of integrin function and cell adhesion. (Mol Cancer Res 2008;6(2):194–204)

## Introduction

Integrins are transmembrane glycoproteins composed of noncovalently linked  $\alpha$  and  $\beta$  subunits. Integrins are essential for cell migration and invasion because they mediate adhesion of cells to the extracellular matrix (ECM) and regulate intracellular signaling pathways that control cytoskeletal organization, force generation, and survival (1). Activated integrins bind to the ECM, cluster at the binding site, and initiate focal adhesions by recruiting cytoplasmic proteins, such as focal adhesion kinase (FAK), c-Src, and paxillin (2). Integrins also activate small GTPase, which in turn activates downstream effector molecules, thereby leading to rearrangement of actin stress fibers and activation of cell adhesion and spreading (3).

Inhibition of the integrin signaling pathway is of great interest in development of drugs for the effective treatment of cancer. Recent research has led to the development of integrin inhibitors that may lead to more effective cancer therapeutics.

Salvicine [4,5-seco-5,10-friedo-abieta-3,4-dihydroxy-5(10),6,8,13-tetraene-11,12-dione] is a diterpenoid quinone compound synthesized by structural modification of a natural product isolated from the traditional Chinese medicinal plant *Salvia prionitis Hance (Labiatae)*. The compound has significant *in vitro* and *in vivo* activity against malignant tumor cells and xenografts, particularly in human solid tumor models (4), and is now in clinical trial in China. Salvicine is a novel DNA topoisomerase inhibitor that directly inhibits DNA topoisomerase (5) and induces the formation of reactive oxygen species (ROS), which in turn modulate DNA damage and repair (6). Salvicine is also antimetastatic and inhibits MDA-MB-435 cell invasion *in vitro* and lung metastasis of MDA-MB-435 orthotopic xenografts *in vivo* (7). Gene expression profiles show that salvicine preferentially inhibits genes relevant to cell adhesion and motility. These genes include the integrins and downstream effector molecules, including FAK, paxillin, and RhoC (7). Salvicine also inhibits the translocation of RhoA and RhoC from the cytosol to the cell membrane (7). Given the emerging correlation between intracellular ROS and integrins, particularly the role of ROS in the regulation of integrin function (8, 9), we propose that salvicine abolishes cell adhesion and subsequent metastasis by inhibiting ROS-driven

Received 4/29/07; revised 9/9/07; accepted 10/15/07.

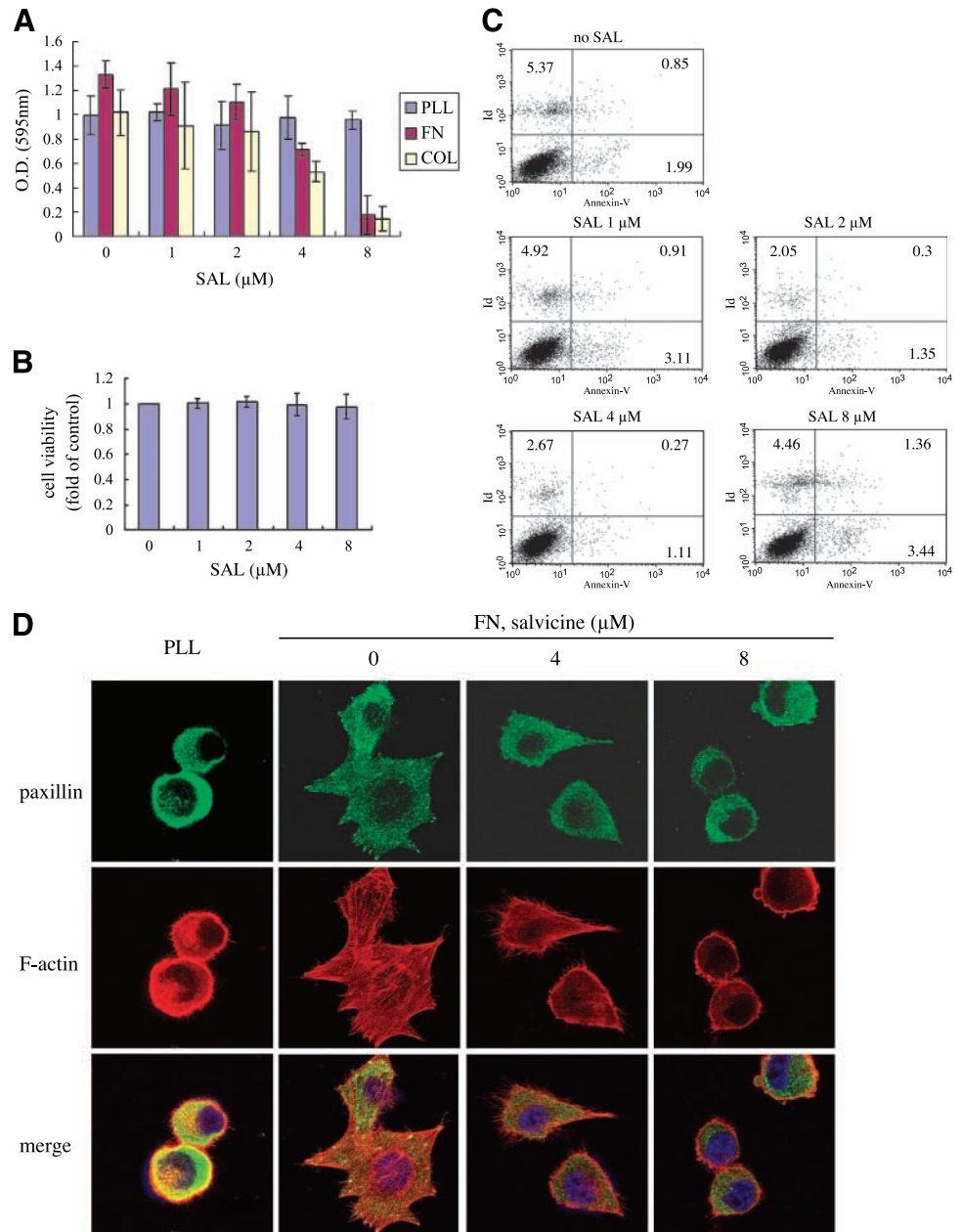
Grant support: National Natural Science Foundation of China grants 30330670, 30600767, and 30721005.

The costs of publication of this article were defrayed in part by the payment of page charges. This article must therefore be hereby marked *advertisement* in accordance with 18 U.S.C. Section 1734 solely to indicate this fact.

Requests for reprints: Jian Ding, Division of Anti-tumor Pharmacology, State Key Laboratory of Drug Research, Shanghai Institute of Materia Medica, Chinese Academy of Sciences, 555 Zu Chong Zhi Road, Zhangjiang Hi-Tech Park, Shanghai 201203, People's Republic of China. Phone: 86-21-50806722; Fax: 86-21-50806722. E-mail: jding@mail.shnc.ac.cn

Copyright © 2008 American Association for Cancer Research.

doi:10.1158/1541-7786.MCR-07-0197



integrin-dependent pathways. The aim of the present study was to investigate the induction of intracellular ROS by salvicine and the involvement of ROS in integrin signaling during cell adhesion and spreading.

## Results

### Salvicine Inhibits Integrin-Mediated Cell Adhesion and Spreading

Our previous studies showed that salvicine strongly inhibits MDA-MB-435 cell invasion *in vitro* and metastasis *in vivo* (7). Cell-ECM adhesion is an essential step in cancer metastasis. For this reason, we investigated the effect of salvicine on MDA-MB-435 cell adhesion to fibronectin and collagen, the most common components of the ECM and typical integrin ligands.

We found that salvicine inhibits cell adhesion in a dose-dependent manner (Fig. 1A). By comparison, cell adhesion to poly-L-lysine, which does not engage with integrins, was not affected. Cell viability was assessed in parallel to determine if the effect of salvicine on cell adhesion was due to cytotoxicity. 3-(4,5-Dimethylthiazol-2-yl)-2,5-diphenyltetrazolium bromide assay showed that MDA-MB-435 cells maintain a high level of viability under the experimental conditions of this investigation (Fig. 1B). We also found that apoptosis was not induced when MDA-MB-435 cells were treated with salvicine for 1 h (Fig. 1C).

Formation of focal adhesion and actin stress fibers is an essential event in cell adhesion and spreading (10). The effect of salvicine on fibronectin-dependent formation of focal

adhesions and actin stress fibers was investigated. MDA-MB-435 cells were plated onto fibronectin-coated or poly-L-lysine-coated glass culture slides in serum-free RPMI 1640. Figure 1B shows fibronectin-induced cell spreading, with focal adhesions localized at the periphery of cells, and well-organized actin stress fibers. By comparison, cells cultured on poly-L-lysine-coated slides maintained a rounded morphology and failed to assemble focal adhesions and stress fibers. Treatment with salvicine dramatically reduced fibronectin-dependent formation of focal adhesion and disrupted actin stress fiber networks. This was accompanied by the rounding up of cells and the retraction of cells from the substratum (Fig. 1D).

#### Salvicine Down-Regulates the Function of $\beta_1$ Integrin

Integrins are the major receptors for ECM proteins. The expression level, affinity for ligands, cell surface distribution,

and downstream signaling of integrins are closely related to the ability of these molecules to initiate cell-ECM attachment. Because  $\alpha_5\beta_1$  integrin is the prototypic fibronectin receptor and  $\alpha_2\beta_1$  integrin is the major receptor for collagen in MDA-MB-435 cells (11), we analyzed the effect of salvicine on the expression levels of  $\alpha_2$ ,  $\alpha_5$ , and  $\beta_1$  integrin subunits in MDA-MB-435 cells. Using flow cytometry, we show that salvicine has no effect on the expression levels of  $\alpha_2$ ,  $\alpha_5$ , or  $\beta_1$  integrin subunits (Fig. 2A). This result suggests that salvicine has an adverse effect on cell adhesion by down-regulating integrin function rather than expression levels. The  $\beta_1$  integrin is common to both the fibronectin and collagen receptors, so the effect of salvicine on  $\beta_1$  integrin activation was investigated using a  $\beta_1$  integrin monoclonal antibody (12G10) that specifically recognizes activated  $\beta_1$  integrin (12, 13). Salvicine treatment inhibited the binding of  $\beta_1$  integrin to

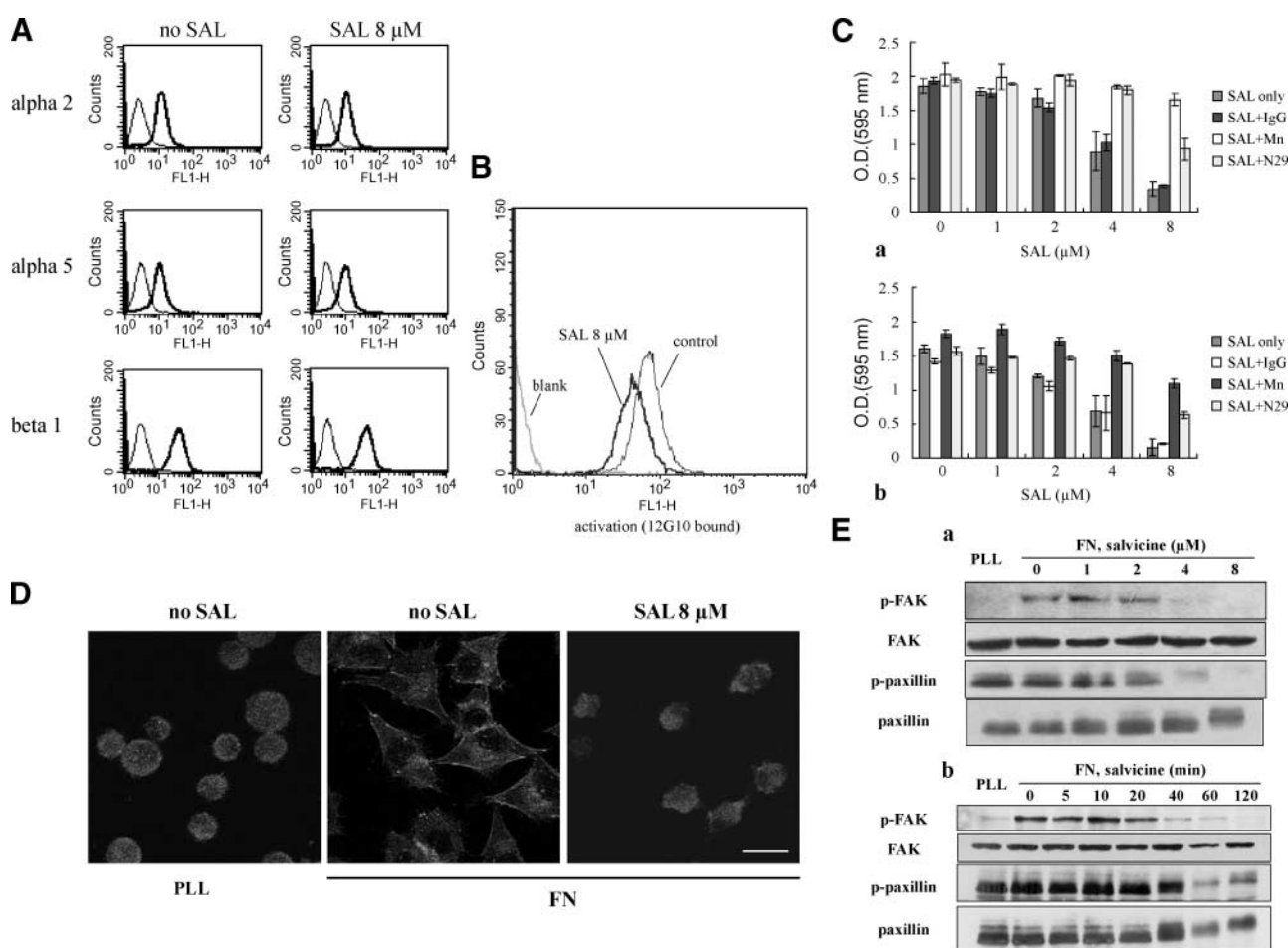


**FIGURE 2.** Salvicine down-regulates  $\beta_1$  integrin function without affecting the expression level of  $\alpha_2$ ,  $\alpha_5$ , or  $\beta_1$  integrin subunits. **A.** Salvicine does not alter the expression level of  $\alpha_2$ ,  $\alpha_5$ , or  $\beta_1$  integrin subunits. Cells were plated and cultured overnight in RPMI 1640 containing 10% fetal bovine serum. The medium was replaced with serum-free RPMI 1640 and cells were incubated with 8  $\mu\text{mol/L}$  salvicine for 1 h. The cells were then incubated with nonspecific mouse IgG (*thin line*) or specific anti- $\alpha_2$ , anti- $\alpha_5$ , or anti- $\beta_1$  integrin antibodies (*thick line*) and detected by flow cytometry. **B.** Salvicine down-regulates the ligand affinity of  $\beta_1$  integrin. Cells were plated onto six-well plates coated with fibronectin or poly-L-lysine in serum-free medium, allowed to adhere for 1 h, and then incubated with various concentrations of salvicine for 1 h. The binding of  $\beta_1$  integrin to 12G10 was detected by flow cytometry. **C.** N29 and  $\text{Mn}^{2+}$  reverse the inhibitory effect of salvicine on cell adhesion. Cells were harvested and seeded onto 96-well plates coated with fibronectin (*a*) or collagen (*b*) in the presence of N29 (5  $\mu\text{g/mL}$ ) or  $\text{Mn}^{2+}$  (1  $\text{mmol/L}$ ). Columns, mean of three independent experiments; bars, SD. **D.** Salvicine inhibits  $\beta_1$  integrin clustering induced by fibronectin. Bar, 20  $\mu\text{m}$ . **E.** Salvicine inhibits the phosphorylation of FAK and paxillin. Cells were seeded on fibronectin-coated plates in serum-free medium, allowed to adhere for 1 h, and then incubated with various concentrations of salvicine (*a*) or for different times (*b*). Phosphorylated FAK (*p-FAK*) and paxillin (*p-paxillin*) were detected by Western blot analysis.

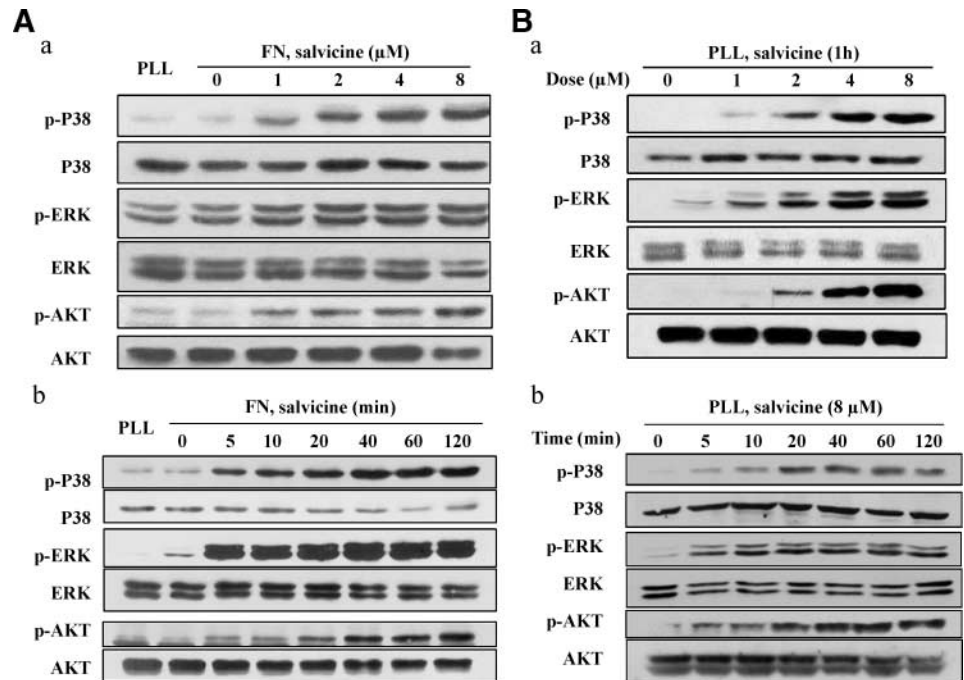


**FIGURE 3.** Salvicine activates ERK, p38 MAPK, and AKT. Cells were plated onto six-well plates coated with fibronectin (**A**) or poly-L-lysine (**B**) in serum-free medium, allowed to adhere for 1 h at 37°C, and then incubated with various concentrations of salvicine (**a**) or for different times with 8  $\mu\text{mol/L}$  salvicine (**b**). Cell lysates were analyzed by Western blot analysis with antibodies against total ERK1/2, p38 MAPK, and AKT or antibodies against the phosphorylated ERK (Thr<sup>202</sup>/Tyr<sup>204</sup>, p-ERK), p38 MAPK (Thr<sup>180</sup>/Tyr<sup>182</sup>; p-P38), and AKT (Ser<sup>473</sup>, p-AKT).

12G10 (Fig. 2B). Moreover, the integrin-activating antibody N29 (14) restored cell adhesion to fibronectin and collagen, with control IgG showing no effect.  $\text{Mn}^{2+}$ , which uniformly activates integrins by inducing an active conformation (15), gave similar results as N29 (Fig. 2C). Together, these results suggest that salvicine down-regulates the ligand affinity of  $\beta_1$  integrin.

When integrins bind to ECM proteins, they become clustered in the plane of the cell membrane and associate with signaling complexes (16). We next tested whether salvicine affects the distribution and downstream signaling of integrins. As shown in Fig. 2D,  $\beta_1$  integrin forms clusters at the cell periphery in the presence of fibronectin, whereas cells grown on poly-L-lysine show an even distribution of  $\beta_1$  integrin. Exposure to salvicine dramatically reduces the clustering of  $\beta_1$  integrin at the cell periphery (Fig. 2D). Correspondingly, the phosphorylation of FAK, an early consequence of the integrin-ligand interaction, was inhibited by salvicine in a dose- and time-dependent manner, with the dephosphorylation of FAK being initiated after 20 min (Fig. 2E). Salvicine also induced the dephosphorylation of paxillin, a key scaffolding protein located at the interface between the cell membrane and the actin cytoskeleton.

#### Salvicine Activates Extracellular Signal-Regulated Kinase and p38 Mitogen-Activated Protein Kinase, Negative Modulators of Fibronectin-Induced Cell Adhesion

The effect of salvicine on the activation status and role of extracellular signal-regulated kinase (ERK), p38 mitogen-activated protein kinase (MAPK), and AKT in integrin-mediated bidirectional signaling was investigated (17, 18). Western blot analysis using antibodies specific to phosphorylated ERK1/2, p38 MAPK, and AKT revealed activation of these proteins by salvicine in a dose-dependent manner

(Fig. 3A). The salvicine-induced phosphorylation of ERK, p38 MAPK, and AKT was initiated after 5 min of exposure to salvicine (Fig. 3A). This is earlier than the observed salvicine-induced dephosphorylation of FAK. Salvicine also induced the phosphorylation of ERK, p38 MAPK, and AKT in the absence of fibronectin (Fig. 3B). This shows that the salvicine-induced activation of ERK, p38 MAPK, and AKT is ECM protein independent.

The role of ERK1/2, p38 MAPK, and AKT in salvicine-inhibited cell adhesion was investigated using specific inhibitors of these signal molecules. Pretreatment with U0126, an inhibitor of the ERK activator MAPK/ERK kinase 1/2, or SB203580, a specific inhibitor of p38 MAPK, partially reversed the inhibition of fibronectin-induced cell adhesion by salvicine, whereas the phosphatidylinositol 3-kinase inhibitor wortmannin had no effect (Fig. 4A). These findings provide evidence that activated ERK and p38 MAPK, rather than AKT, are involved in the inhibition of cell adhesion by salvicine.

#### Activated ERK and p38 MAPK Negatively Regulate $\beta_1$ Integrin Function

The down-regulation of  $\beta_1$  integrin function by activated ERK and p38 MAPK was investigated. Pretreatment with U0126 or SB203580 partially reversed the inhibitory effect of salvicine on the binding of  $\beta_1$  integrin to 12G10 (Fig. 4B). U0126 and SB203580 also restored  $\beta_1$  integrin clustering in salvicine-treated cells (Fig. 4C) and lead to partial restoration of FAK phosphorylation (Fig. 4D). By comparison, pretreatment with U0126 or SB203580 did not restore disrupted actin stress fiber networks or reverse the cell morphology induced by salvicine (Fig. 4C). These results suggest that the disruption of the actin stress fiber networks is not attributed to the down-regulation of  $\beta_1$  integrin function.

### Salvicine Activates ERK and p38 MAPK in a ROS-Dependent Manner

Our previous study found that salvicine stimulated intracellular ROS production in human breast cancer MCF-7 cells (6). There is also evidence that oxidants activate MAPK signaling pathways (19). These findings lead us to investigate the mechanism underlying the salvicine-induced activation of ERK and p38 MAPK and to determine the role of ROS in this process. ROS production in MDA-MB-435 cells was assessed following exposure to salvicine. We found that salvicine increased the level of ROS in a time-dependent manner with ROS generation starting after 5 min of exposure to salvicine and peaking at 60 min (Fig. 5A). Such an increase in

intracellular oxidants, revealed by the redox-sensitive fluorescent dye 2,7-dichlorodihydrofluorescein diacetate, is most likely due to hydrogen peroxide to which this probe is selectively sensitive.

Two approaches were used to determine if ROS induced the activation of ERK and p38 MAPK. First, we examined the activation status of these pathways under oxidative stress by exposing MDA-MB-435 cells to hydrogen peroxide. Second, we used *N*-acetyl-L-cysteine (NAC), a well-recognized ROS scavenger, to decrease the intracellular level of ROS (Fig. 5B). Phosphorylation of ERK and p38 MAPK increased significantly after 5 min of exposure to hydrogen peroxide and was maintained for 2 h (Fig. 5C). The time course of ERK and p38

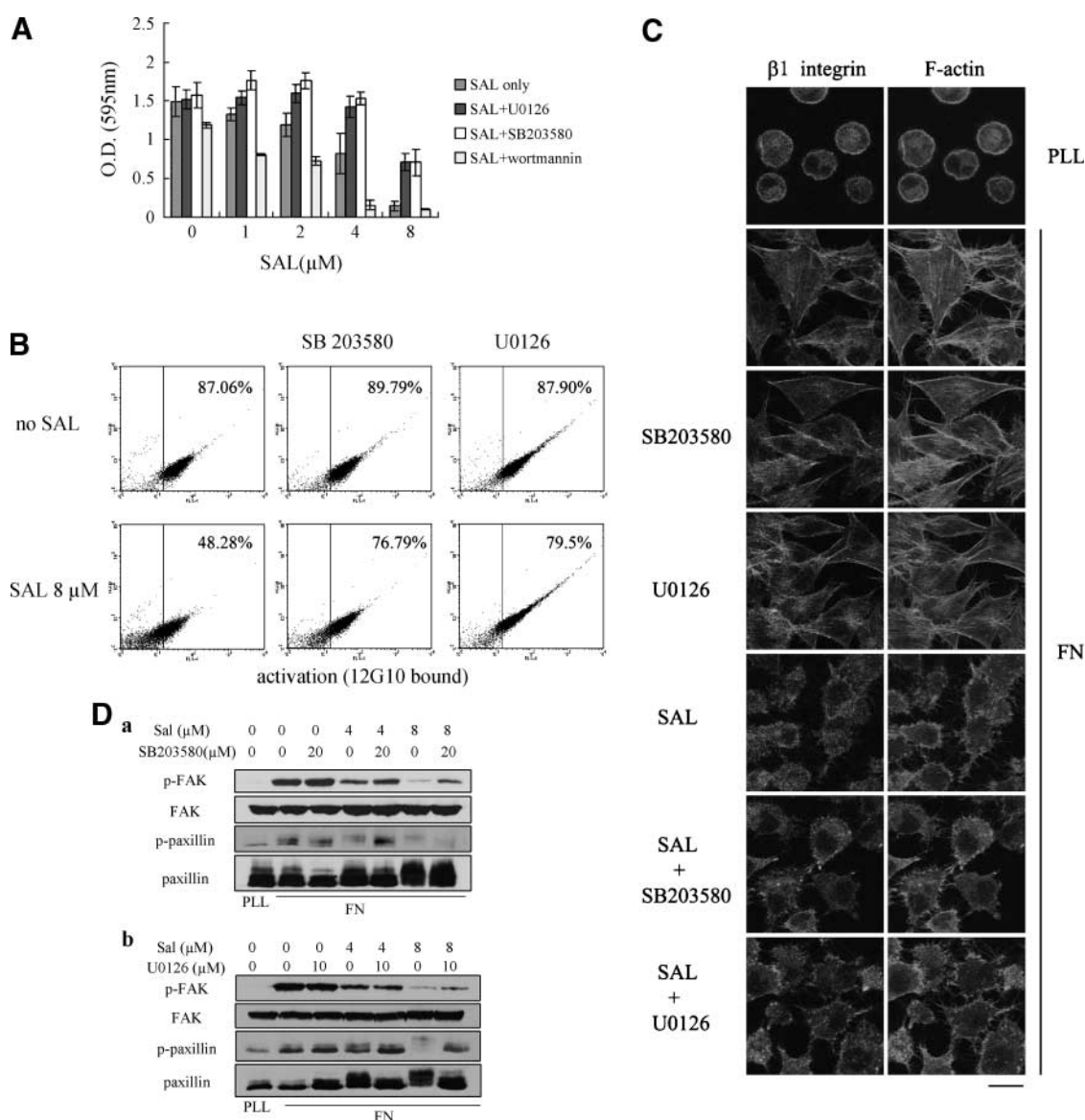


**FIGURE 4.** Salvicine down-regulates cell adhesion and  $\beta_1$  integrin function by ERK and p38 MAPK signaling. Cells were pretreated with SB203580 (20  $\mu$ mol/L), U0126 (10  $\mu$ mol/L), or wortmannin (1  $\mu$ mol/L) for 30 min before the addition of salvicine. **A.** Effect of SB203580, U0126, and wortmannin on the inhibition of fibronectin-induced cell adhesion by salvicine. Columns, mean of three independent experiments; bars, SD. **B.** Effect of SB203580 and U0126 on the reduction of  $\beta_1$  integrin ligand affinity by salvicine. **C.** Effect of U0126 and SB203580 on the reduction of  $\beta_1$  integrin clusters by salvicine. Bar, 20  $\mu$ m. **D.** Effect of SB203580 and U0126 on the salvicine-inhibited phosphorylation of FAK and paxillin.

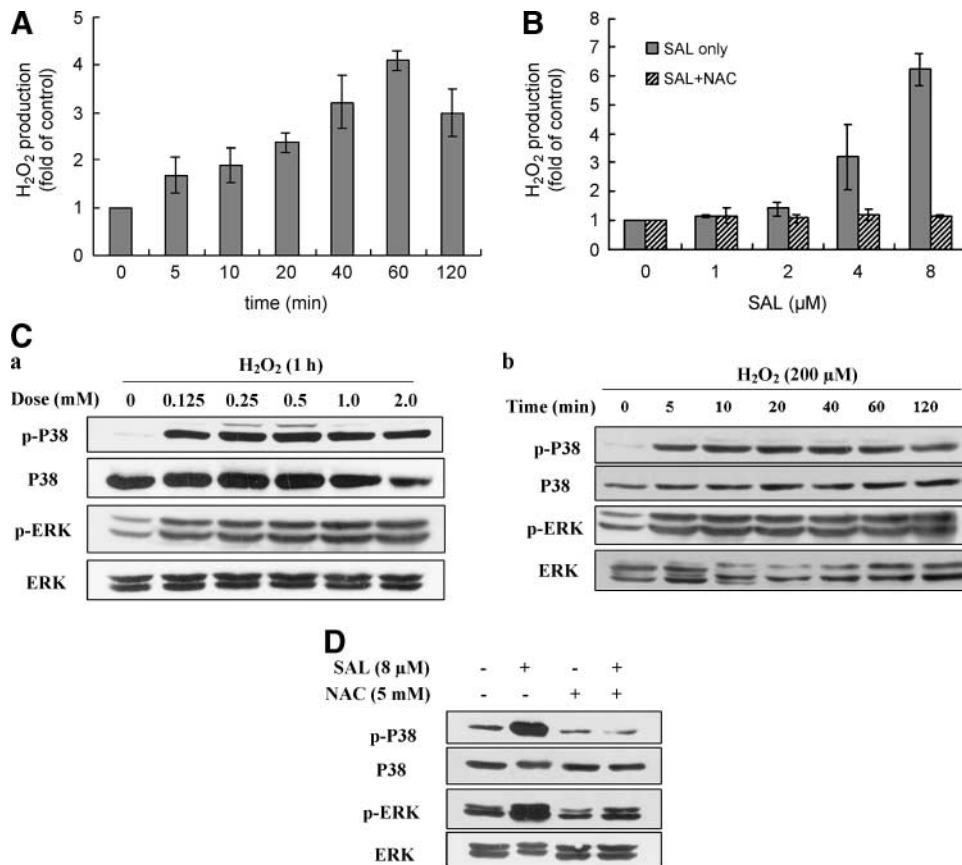


**FIGURE 5.** Salvicine activates ERK and p38 MAPK in a ROS-dependent manner. **A.** Salvicine induces an increase in the level of ROS in a time-dependent manner. Cells were seeded onto six-well plates and cultured overnight. The complete medium was replaced with serum-free medium and cells were incubated with 8  $\mu\text{mol/L}$  salvicine for different times. The intracellular ROS level was detected by flow cytometry. **B.** NAC reverses salvicine-induced ROS generation. Cells were pretreated with 5 mmol/L NAC for 30 min before exposure to 8  $\mu\text{mol/L}$  salvicine. The intracellular hydrogen peroxide level was measured after 1 h of incubation. Columns, mean of three independent experiments; bars, SD. **C.** Hydrogen peroxide induced an increase in the phosphorylation of ERK and p38 MAPK in a dose-dependent (a) and time-dependent (b) manner. Cells were seeded onto six-well plates and cultured overnight. The complete medium was replaced with serum-free medium and cells were incubated with various concentrations of hydrogen peroxide or for different times with 200  $\mu\text{mol/L}$  hydrogen peroxide. **D.** NAC reverses salvicine-induced phosphorylation of ERK and p38 MAPK. Cells were pretreated with 5 mmol/L NAC for 30 min before the exposure of cells to 8  $\mu\text{mol/L}$  salvicine.

MAPK activation by hydrogen peroxide is similar to that observed for salvicine. The reversal of salvicine-induced activation of ERK and p38 MAPK by NAC confirms the involvement of ROS in this process (Fig. 5D). Together, these results show that salvicine activates ERK and p38 MAPK by up-regulating the intracellular level of ROS.

#### *ROS Inactivates $\beta_1$ Integrin and Reduces Integrin-Mediated Cell Adhesion*

Our data suggest a correlation between salvicine-induced production of ROS and the inhibition of  $\beta_1$  integrin function. Salvicine induces ROS production, which activates ERK and p38 MAPK, and in turn, activated ERK and p38 MAPK down-regulate  $\beta_1$  integrin ligand affinity and inhibit fibronectin-induced cell adhesion. We used NAC to determine if the inhibitory effect of salvicine on  $\beta_1$  integrin ligand affinity and cell adhesion was ROS dependent. Pretreatment with 5 mmol/L NAC reversed the inhibitory effect of salvicine on  $\beta_1$  integrin ligand affinity (Fig. 6A) and restored the adhesion capacity of MDA-MB-435 cells (Fig. 6B). NAC pretreatment also had a

protective effect on the integrity of the actin stress fiber networks and fibronectin-stimulated cell spreading in the presence of salvicine (Fig. 6C). These results indicate a causative role of ROS in the salvicine-induced down-regulation of  $\beta_1$  integrin ligand affinity and cell-ECM adhesion. We also found that hydrogen peroxide significantly decreased the binding of  $\beta_1$  integrin to 12G10 (Fig. 6D), suggesting inactivation of  $\beta_1$  integrin ligand affinity by hydrogen peroxide. Hydrogen peroxide also inhibited  $\beta_1$  integrin-dependent cell adhesion (Fig. 6E). NAC reversed both inhibitory effects of hydrogen peroxide (Fig. 6D and E). Together, these findings confirm a significant role of ROS in the negative regulation of  $\beta_1$  integrin ligand affinity and integrin-dependent cell adhesion.

#### *Salvicine Inhibits RhoA Activity in a ROS-Dependent Manner*

Our data showed that NAC, but not U0126 and SB203580, protects the actin stress fiber networks and cell morphology from the inhibitory effect of salvicine. In addition, the reversal of salvicine-induced inhibition of cell adhesion was more

pronounced for NAC than for U0126 and SB203580. This suggests that other downstream effectors of ROS participate in the salivine-induced disruption of the actin cytoskeleton and inhibition of cell adhesion. RhoA is a key regulator of actin

cytoskeleton formation and seems from our following results to be a downstream effector of ROS. Treatment of MDA-MB-435 cells with 8  $\mu\text{mol/L}$  salivine reduced RhoA activity (Fig. 7A), and this effect was reversed by NAC pretreatment (Fig. 7B).

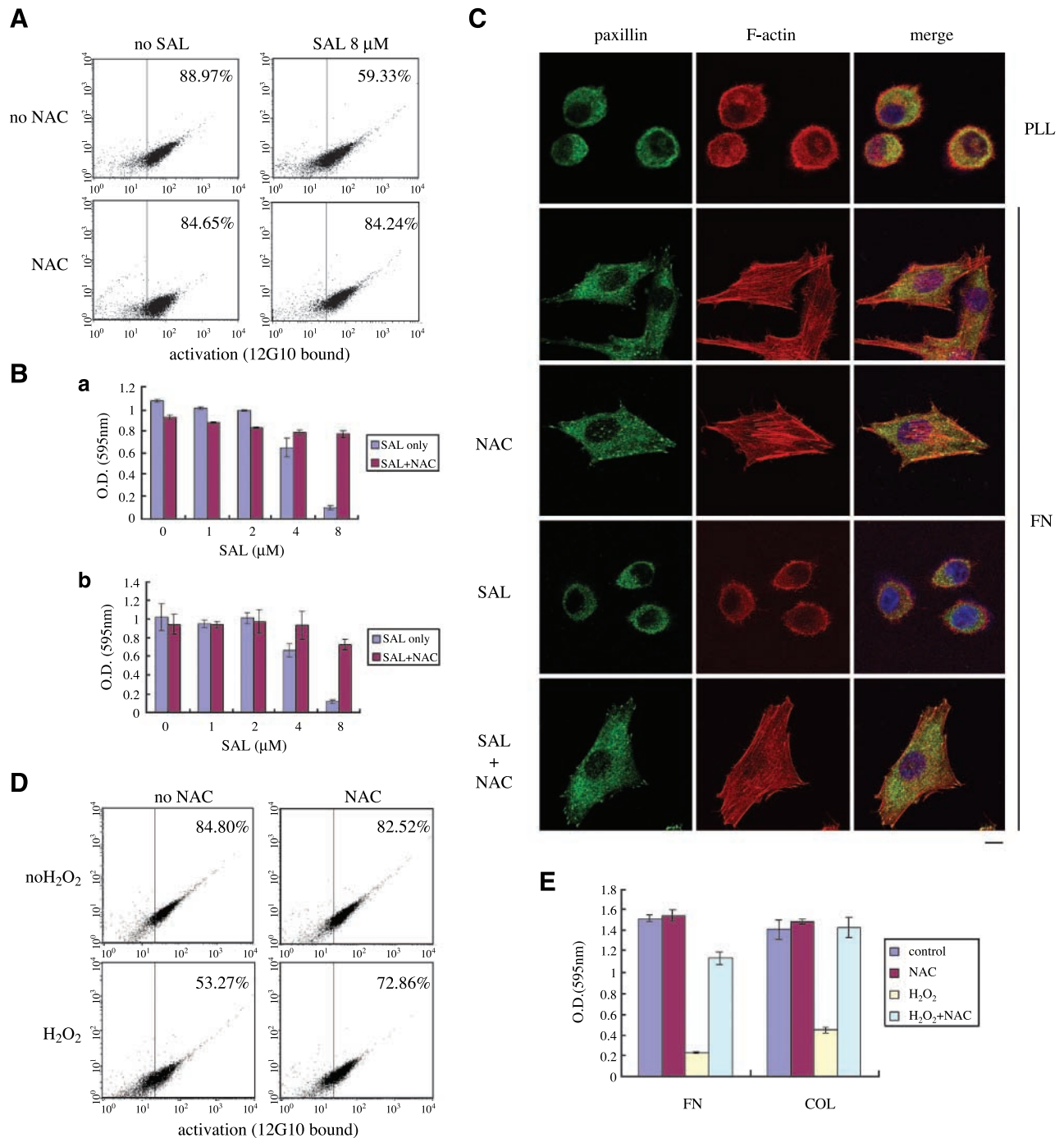


**FIGURE 6.** Salivine inactivates  $\beta_1$  integrin in a ROS-dependent manner. **A.** Effect of NAC on salivine-induced inhibition of  $\beta_1$  integrin ligand affinity. **B.** Effect of NAC on salivine-induced inhibition of cell attachment to fibronectin (a) and collagen (b). Columns, mean of three independent experiments; bars, SD. **C.** Effect of NAC on salivine-induced disruption of focal adhesions and actin stress fibers. Bar, 8  $\mu\text{m}$ . **D.** Inhibition of  $\beta_1$  integrin ligand affinity by hydrogen peroxide. The ligand affinity of  $\beta_1$  integrin was inactivated in cells exposed to 200  $\mu\text{mol/L}$  hydrogen peroxide for 1 h. Hydrogen peroxide–induced inhibition of  $\beta_1$  integrin ligand affinity was reversed by pretreatment of cells with 5 mmol/L NAC. **E.** Inhibition of cell adhesion by hydrogen peroxide.  $\beta_1$  Integrin-dependent cell adhesion was inhibited by 200  $\mu\text{mol/L}$  hydrogen peroxide. Columns, mean of three independent experiments; bars, SD.

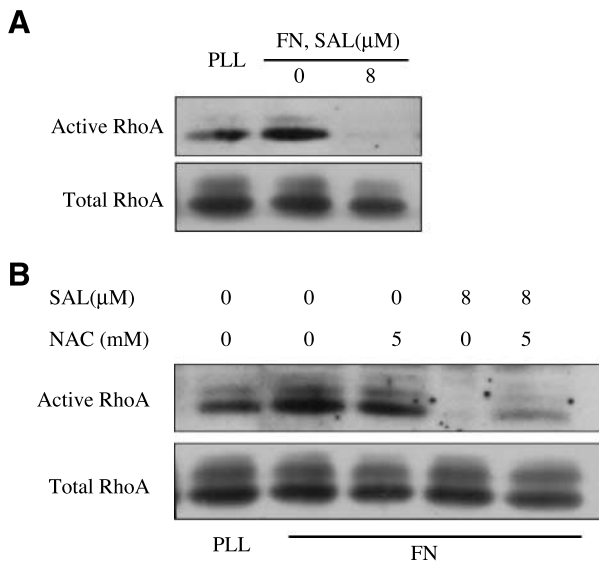


**FIGURE 7.** Salvicine inhibits RhoA activity in a ROS-dependent manner. Cells were seeded onto fibronectin-coated or poly-L-lysine-coated culture dishes, allowed to adhere for 1 h at 4°C, and then incubated with 8  $\mu$ mol/L salvicine for 1 h. **A.** Salvicine inhibits RhoA activity. **B.** Effect of NAC on the salvicine-reduced activity of RhoA. Cells were pretreated with 5 mmol/L NAC for 30 min before salvicine was added.

## Discussion

Our previous studies show that salvicine, a novel diterpenoid quinone compound, significantly reduces the metastatic potential of MDA-MB-435 cells both *in vitro* and *in vivo*. Mechanistic studies indicate that the antimetastatic effect of salvicine is closely related to the Rho pathway (7). In the present study, we show that salvicine down-regulates  $\beta_1$  integrin function and inhibits cell-ECM attachment, thereby providing further clues to the mechanism underlying the antimetastatic efficacy of salvicine.

$\beta_1$  Integrin plays a significant role in tumor metastasis by mediating metastatic tumor cell adhesion and extravasation at the target organ (20, 21). This is supported by the over-expression of the active conformation of  $\beta_1$  integrin in vulvar squamous cell carcinomas (22) and by the encapsulation and less invasive nature of  $\beta_1$  integrin knockdown tumors *in vivo* (22). In the present study, the positive interaction between  $\beta_1$  integrin and the 12G10 monoclonal antibody shows that  $\beta_1$  integrin is maintained in the active conformation in MDA-MB-435 cells. Reversal of this interaction by salvicine suggests that the antimetastatic capacity of salvicine is  $\beta_1$  integrin dependent. ROS, including hydrogen peroxide, hydroxyl radical, and superoxide anions, are important signaling molecules and mediate a wide range of cellular responses, such as proliferation, differentiation, apoptosis, and adhesion, under pathophysiologic and physiologic conditions (23-25). ROS-induced activation of cell adhesion is due to the inhibition by ROS of the low molecular weight phosphotyrosine phosphatase and the subsequent phosphorylation of FAK (25, 26). Conversely, recent reports highlight an inhibitory role of ROS in the regulation of integrin function and the cytoskeleton (27, 28). ROS-induced inactivation of integrins is commonly investigated using antioxidants. The antioxidant NAC promotes cell

adhesion by increasing the thiol expression of  $\beta_1$  integrin (8). The antioxidant DTT is also used to further understand the responsive role of ROS in the regulation of  $\alpha_L\beta_2$  integrins (9). The present study showed that NAC abrogates salvicine-induced ROS generation and reverses the effect of salvicine on cell adhesion and spreading. Similar effects by hydrogen peroxide were also reversed by NAC. Together, these findings show that the negative regulation of cell adhesion driven by salvicine is ROS dependent. Similarly, we show that NAC reverses the salvicine-induced and hydrogen peroxide-induced inhibition of  $\beta_1$  integrin ligand affinity. These data provide direct evidence for the involvement of ROS in salvicine-mediated  $\beta_1$  integrin inactivation.

ROS acts as a signaling molecule in the activation of several pathways, including the MAPK and AKT pathways (19). The involvement of the MAPK and AKT pathways in salvicine-driven ROS-mediated function was investigated using U0126, SB203580, and wortmannin, specific inhibitors of MAPK/ERK kinase, p38 MAPK, and phosphatidylinositol 3-kinase, respectively. Both U0126 and SB203580 partially reversed the salvicine-induced inhibition of cell adhesion to fibronectin and the salvicine-induced inhibition of  $\beta_1$  integrin affinity for 12G10, the monoclonal antibody specific for active  $\beta_1$  integrin. By comparison, wortmannin had no effect. These results suggest that ERK and p38 MAPK function as ROS effectors and are responsible for the salvicine-induced inhibition of integrin function and cell attachment.

Although it is generally accepted that p38 MAPK plays a role in the regulation of integrin function and cell adhesion, this role of p38 MAPK has not been widely studied (29, 30). A recent study reported that the p38-dependent phosphorylation of  $\beta_1$  integrin at Ser<sup>785</sup> was critical for adhesion of the T-cell lymphoma line Karpas299 to fibronectin and collagen. However, this phenomenon was highly cell type specific (31). Other issues, however, stand quite in contrast to this case and gave a clue that p38 MAPK may inhibit  $\beta_1$  integrin function (32). In our study, the findings that SB203580 reversed salvicine-induced inhibition of  $\beta_1$  integrin ligand affinity and phosphorylation of FAK offer the firsthand evidence that p38 MAPK mediates inhibition of cell adhesion to matrix proteins by inhibiting  $\beta_1$  integrin function. The Ras-Raf-ERK pathway is also involved in the inactivation of integrins, including  $\alpha_{IIb}\beta_3$  and  $\alpha_5\beta_1$  integrins (33, 34). An investigation of the mechanism underlying the Ras-Raf-ERK pathway shows that activation and cytoplasmic localization of ERK are required for suppression of  $\alpha_5\beta_1$  integrin activation (34).

RhoA is a key regulator of actin stress fibers (35). We previously showed that salvicine inhibits the membrane translocation of RhoA (7). Consistent with this finding, our present study shows that salvicine significantly reduces the level of GTP-bound RhoA. These salvicine-induced changes would enhance the disruption of actin stress fiber networks. NAC pretreatment protects the actin stress fiber network and cell morphology from salvicine-induced damage, with U0126 or SB203580 showing no effect. Furthermore, the protective effect of NAC on salvicine-induced inhibition of cell adhesion was greater than that of U0126 or SB203580. These results suggest that RhoA is a downstream effector of ROS linked to cytoskeleton disruption. These results are supported by



previous findings that ROS inactivates low molecular weight phosphotyrosine phosphatase and phosphorylates p190Rho-GAP to trigger the hydrolysis of GTP-bound RhoA (36). There is positive feedback between RhoA and integrins (37) that drives the activation and clustering of integrins, the phosphorylation of FAK and paxillin, and enhancement of cell adhesion (38, 39). Together, these findings strongly suggest that salvicine-induced disruption of actin stress fiber is mainly attributed to the ROS-dependent inhibition of RhoA activity; this, in turn, negatively regulates integrin function and cell adhesion.

In summary, these findings of the present study provide a better understanding of the molecular mechanisms underlying the antimetastatic activity of salvicine. The indirect action of ROS-MAPK- $\beta_1$  integrin provides clues to the function of ROS upstream of the integrins in the molecular pathways underlying salvicine-associated antimetastatic activity. Our identification of p38 MAPK as a putative regulator in integrin-mediated cancer metastasis provides a basis for future investigations.

## Materials and Methods

### Drugs and Reagents

Tangerine yellow crystalloid salvicine was kindly provided by Professor Jin-Sheng Zhang (Department of Phytochemistry, Shanghai Institute of Materia Medica, Chinese Academy of Sciences, Shanghai, People's Republic of China). Salvicine was structurally modified from the lead compound isolated from the Chinese medicinal plant *S. prionitis*. The end product was purified by column chromatography on a silica gel eluted with a cyclohexane-ethyl acetate mixture (4:1, v/v) to produce salvicine (65% yield). Purity was >99.8%, as determined by high-performance liquid chromatography (40). Salvicine dissolved in DMSO at 0.05 mol/L was used as a stock solution and maintained at  $-20^{\circ}\text{C}$  in the dark. Aliquots were thawed just before each experiment and diluted to the desired concentration with saline. Poly-L-lysine, collagen, fibronectin, and 2,7-dichloro-rodihydrofluorescein diacetate were obtained from Sigma-Aldrich. Antibodies against FAK and paxillin and FITC-conjugated antibodies against  $\alpha_2$ ,  $\alpha_5$ , or the  $\beta_1$  integrin subunit were purchased from Santa Cruz Biotechnology. The  $\beta_1$  integrin-activating antibody (clone N29) was obtained from Chemicon. The antibodies against ERK1/2, p38 MAPK, and AKT and phosphospecific antibodies to ERK1/2 (Thr<sup>202</sup>/Tyr<sup>204</sup>), p38 MAPK (Thr<sup>180</sup>/Tyr<sup>182</sup>), and AKT (Ser<sup>473</sup>) were obtained from Cell Signaling Technology. Phosphospecific antibodies to FAK (Tyr<sup>397</sup>) and paxillin (Tyr<sup>118</sup>) were obtained from Biosource International. Alexa Fluor 488 goat anti-rabbit IgG, Alexa Fluor 488 goat anti-mouse IgG, and Alexa Fluor 532 phalloidin were obtained from Molecular Probes. U0126, SB203580, and wortmannin were purchased from Calbiochem.

### Cell Culture

The human breast cancer cell line MDA-MB-435 was obtained from the American Type Culture Collection. Cells were maintained in RPMI 1640 (Invitrogen) supplemented with 10% (v/v) heat-inactivated fetal bovine serum, 2 mmol/L L-glutamine, 100 units/mL penicillin, 100  $\mu\text{g}/\text{mL}$  streptomycin,

and 0.25  $\mu\text{g}/\text{mL}$  amphotericin B. Cells were cultured in a humidified atmosphere containing 5%  $\text{CO}_2$  at  $37^{\circ}\text{C}$ .

### Cell Adhesion Assay

The cell adhesion assay was done as previously described (41). Briefly, fibronectin, collagen, or poly-L-lysine was diluted in sterile water and applied to 96-well plates overnight at  $4^{\circ}\text{C}$ . Nonspecific binding sites were blocked with 1% bovine serum albumin for 1 h at room temperature. Cells were serum starved for 45 min, detached with 2 mmol/L EDTA in PBS, plated in triplicate onto wells in serum-free medium with or without salvicine or hydrogen peroxide, and allowed to adhere for 1 h at  $37^{\circ}\text{C}$ . Nonadherent cells were washed away and adherent cells were fixed with 4% paraformaldehyde and stained with 0.1% crystal violet in 2% methanol. Following extensive washing with tap water, dye was extracted with 10% acetic acid and quantified by measuring absorbance at 595 nm on a multiwell spectrophotometer (VersaMax, Molecular Devices).

The effect of U0126, SB203580, wortmannin, or NAC on salvicine-inhibited cell adhesion was investigated by adding the inhibitors 30 min before the cells were detached.

### Immunofluorescence

Cells were plated onto glass culture slides coated with fibronectin or poly-L-lysine in serum-free medium, allowed to adhere for 1 h, and then incubated with various concentrations of salvicine for various times with or without pretreatment with SB203580, U0126, or NAC for 30 min. Cells were fixed with 4% paraformaldehyde and permeabilized with PBS containing 0.1% Triton X-100. After blocking with 5% bovine serum albumin for 30 min, cells were incubated with primary antibodies for 1 h, washed thrice with PBS, and then incubated with the Alexa Fluor 488-conjugated secondary antibodies in the dark. Cells were incubated with Alexa Fluor 532-conjugated phalloidin to stain stress fibers. The nuclei were visualized by staining with 0.5  $\mu\text{g}/\text{mL}$  4',6-diamidino-2-phenylindole. Pictures were obtained using a Leica TCS confocal microscope (Leica Microsystems, Inc.).

### Analysis of Cell Viability

Cell viability was assessed using the 3-(4,5-dimethylthiazol-2-yl)-2,5-diphenyltetrazolium bromide assay. Cells were seeded onto 96-well plates precoated with fibronectin. After 1 h of attachment, salvicine was added in a total volume of 10  $\mu\text{L}$  at the desired concentration. The medium was replaced with fresh RPMI 1640 after 1 h and then 20  $\mu\text{L}$  of 5 mg/mL 3-(4,5-dimethylthiazol-2-yl)-2,5-diphenyltetrazolium bromide (Sigma Chemical) were added to each well. The plates were then incubated at  $37^{\circ}\text{C}$  for 4 h. Next, 100  $\mu\text{L}$  of triplex solution (10% SDS, 5% isobutanol, and 12 mmol/L HCl) were added, and cells were incubated at  $37^{\circ}\text{C}$  for an additional 12 h. The absorbance was measured at 570 nm using a multiwell spectrophotometer.

### Determination of Apoptotic Cells

Cells were seeded onto fibronectin-coated six-well plates in serum-free RPMI 1640. Following 1 h of attachment, salvicine was added at a range of concentrations. After 1 h of incubation,

the level of apoptotic cells was quantified using an Annexin V-FITC apoptosis detection kit (BD Biosciences). Briefly, cells were resuspended in cold binding buffer and then incubated for 15 min in the dark at room temperature following the addition of 5  $\mu$ L of Annexin V-FITC and 5  $\mu$ L of propidium iodide. Flow cytometry analysis was done using a flow cytometer (FACSCalibur, BD Biosciences).

#### Expression of Cell Surface Integrins

Cells were seeded onto six-well plates in complete medium and cultured overnight. The growth medium was then replaced with serum-free RPMI 1640, and the cells were incubated in the presence of 8  $\mu$ mol/L salvicine for 1 h. Cells were detached, washed with 5% bovine serum albumin thrice, and incubated on ice for 1 h with FITC-conjugated antibody against  $\alpha_2$ ,  $\alpha_5$ , or the  $\beta_1$  integrin subunit. The cells were then washed thrice and resuspended in ice-cold PBS. The fluorescence intensity was measured with a flow cytometer.

#### 12G10 Binding

Cells were plated onto fibronectin-coated six-well plates in serum-free medium, allowed to adhere for 1 h at 37°C, and then incubated with 8  $\mu$ mol/L salvicine for 1 h with or without pretreatment with SB203580, U0126, or NAC for 30 min. Cells were washed with PBS, detached with trypsin, resuspended in 100  $\mu$ L of 5% bovine serum albumin, and incubated for 1 h on ice with anti-active  $\beta_1$  integrin antibody 12G10 (Serotec). Cells were washed thrice and then incubated with goat anti-mouse Alexa Fluor 488–conjugated secondary antibodies for 1 h in the dark. The fluorescence intensity was detected with a flow cytometer.

#### Western Blot Analysis

Cells were washed twice with ice-cold PBS and then lysed on ice for 30 min in lysis buffer [2 mmol/L sodium orthovanadate, 50 mmol/L NaF, 20 mmol/L HEPES (pH 7.5), 150 mmol/L NaCl, 1.5 mmol/L  $MgCl_2$ , 5 mmol/L sodium pyrophosphate, 10% glycerol, 0.2% Triton X-100, 5 mmol/L EDTA, 1 mmol/L phenylmethylsulfonyl fluoride, 10  $\mu$ g/mL leupeptin, 10  $\mu$ g/mL aprotinin]. Lysates were clarified by centrifugation at 14,000  $\times$  g for 10 min at 4°C. Equal amounts of protein were subjected to SDS-PAGE and transferred to nitrocellulose membranes (Amersham Pharmacia Biotech). The membranes were blocked with 5% nonfat milk in TBS-Tween 20 for 1 h at room temperature and then probed with primary antibodies overnight at 4°C. After incubation with horseradish peroxidase–conjugated secondary antibodies, the immunoreactive bands were visualized by the SuperSignal West Pico Chemiluminescent kit (Pierce).

#### Intracellular Hydrogen Peroxide Measurement

Intracellular hydrogen peroxide measurement was done as previously described (6). Briefly, the cells were seeded onto six-well plates and cultured overnight. The complete culture medium was replaced with serum-free RPMI 1640, and then cells were incubated with various concentrations of salvicine or for different times with 8  $\mu$ mol/L salvicine, with or without pretreatment with 5 mmol/L NAC. 2,7-Dichloro-rodihydrofluorescein diacetate at a final concentration of 10  $\mu$ mol/L was added

15 min before the end of the incubation. Cells were washed twice with ice-cold PBS. The samples were kept on ice in the dark for immediate detection using a flow cytometer.

#### RhoA Activity

Cells were seeded onto fibronectin-coated or poly-L-lysine–coated culture dishes, allowed to adhere for 1 h at 37°C, and then incubated with 8  $\mu$ mol/L salvicine for 1 h. Cells were washed with ice-cold PBS and then lysed in ice-cold lysis buffer [25 mmol/L HEPES (pH 7.5), 150 mmol/L NaCl, 1% Igepal CA-630, 10 mmol/L  $MgCl_2$ , 1 mmol/L EDTA, 10% glycerol, 1 mmol/L phenylmethylsulfonyl fluoride, 10  $\mu$ g/mL leupeptin, 10  $\mu$ g/mL aprotinin]. The lysates were clarified by centrifugation at 14,000  $\times$  g at 4°C for 5 min. Rhotekin RBD agarose (Upstate) was added to the supernatant and incubated for 45 min at 4°C with gentle agitation. The agarose beads were collected by centrifugation, washed, and then boiled in loading buffer for 5 min. The protein samples were analyzed by Western blot.

#### References

- Hood JD, Cheresch DA. Role of integrins in cell invasion and migration. *Nat Rev Cancer* 2002;2:91–100.
- Huang Q, Shen HM, Shui G, Wenk MR, Ong CN. Emodin inhibits tumor cell adhesion through disruption of the membrane lipid Raft-associated integrin signaling pathway. *Cancer Res* 2006;66:5807–15.
- Salsmann A, Schaffner-Reckinger E, Kabile F, Plancon S, Kieffer N. A new functional role of the fibrinogen RGD motif as the molecular switch that selectively triggers integrin  $\alpha$ IIb $\beta$ 3-dependent RhoA activation during cell spreading. *J Biol Chem* 2005;280:33610–9.
- Qing C, Zhang JS, Ding J. *In vitro* cytotoxicity of salvicine, a novel diterpenoid quinone. *Zhongguo Yao Li Xue Bao* 1999;20:297–302.
- Meng LH, Zhang JS, Ding J. Salvicine, a novel DNA topoisomerase II inhibitor, exerting its effects by trapping enzyme-DNA cleavage complexes. *Biochem Pharmacol* 2001;62:733–41.
- Lu HR, Zhu H, Huang M, et al. Reactive oxygen species elicit apoptosis by concurrently disrupting topoisomerase II and DNA-dependent protein kinase. *Mol Pharmacol* 2005;68:983–94.
- Lang JY, Chen H, Zhou J, et al. Antimetastatic effect of salvicine on human breast cancer MDA-MB-435 orthotopic xenograft is closely related to Rho-dependent pathway. *Clin Cancer Res* 2005;11:3455–64.
- Laragione T, Bonetto V, Casoni F, et al. Redox regulation of surface protein thiols: identification of integrin  $\alpha$ -4 as a molecular target by using redox proteomics. *Proc Natl Acad Sci U S A* 2003;100:14737–41.
- Edwards BS, Curry MS, Southon EA, Chong AS, Graf LH, Jr. Evidence for a dithiol-activated signaling pathway in natural killer cell avidity regulation of leukocyte function antigen-1: structural requirements and relationship to phorbol ester- and CD16-triggered pathways. *Blood* 1995;86:2288–301.
- Carragher NO, Frame MC. Focal adhesion and actin dynamics: a place where kinases and proteases meet to promote invasion. *Trends Cell Biol* 2004;14:241–9.
- Maemura M, Akiyama SK, Woods VL, Jr, Dickson RB. Expression and ligand binding of  $\alpha$ 2 $\beta$ 1 integrin on breast carcinoma cells. *Clin Exp Metastasis* 1995;13:223–35.
- Ng T, Shima D, Squire A, et al. PKC $\alpha$  regulates  $\beta$ 1 integrin-dependent cell motility through association and control of integrin traffic. *EMBO J* 1999;18:3909–23.
- Zetser A, Bashenko Y, Miao HQ, Vlodavsky I, Ilan N. Heparanase affects adhesive and tumorigenic potential of human glioma cells. *Cancer Res* 2003;63:7733–41.
- Mould AP, Travis MA, Barton SJ, et al. Evidence that monoclonal antibodies directed against the integrin  $\beta$  subunit plexin/semaphorin/integrin domain stimulate function by inducing receptor extension. *J Biol Chem* 2005;280:4238–46.
- Takagi J, Petre BM, Walz T, Springer TA. Global conformational rearrangements in integrin extracellular domains in outside-in and inside-out signaling. *Cell* 2002;110:599–11.

16. Hehlhans S, Haase M, Cordes N. Signalling via integrins: implications for cell survival and anticancer strategies. *Biochim Biophys Acta* 2007;1775:163–80.
17. Giancotti FG, Ruoslahti E. Integrin signaling. *Science* 1999;285:1028–32.
18. Hughes PE, Pfaff M. Integrin affinity modulation. *Trends Cell Biol* 1998;8:359–64.
19. Sugden PH, Clerk A. Oxidative stress and growth-regulating intracellular signaling pathways in cardiac myocytes. *Antioxid Redox Signal* 2006;8:2111–24.
20. Heyder C, Gloria-Maercker E, Hatzmann W, Niggemann B, Zanker KS, Dittmar T. Role of the  $\beta$ 1-integrin subunit in the adhesion, extravasation and migration of T24 human bladder carcinoma cells. *Clin Exp Metastasis* 2005;22:99–106.
21. Enns A, Gassmann P, Schluter K, et al. Integrins can directly mediate metastatic tumor cell adhesion within the liver sinusoids. *J Gastrointest Surg* 2004;8:1049–59.
22. Brockbank EC, Bridges J, Marshall CJ, Sahai E. Integrin  $\beta$ 1 is required for the invasive behaviour but not proliferation of squamous cell carcinoma cells *in vivo*. *Br J Cancer* 2005;92:102–12.
23. Hancock JT, Desikan R, Neill SJ. Role of reactive oxygen species in cell signalling pathways. *Biochem Soc Trans* 2001;29:345–50.
24. Finkel T. Oxidant signals and oxidative stress. *Curr Opin Cell Biol* 2003;15:247–54.
25. Ben Mahdi MH, Andrieu V, Pasquier C. Focal adhesion kinase regulation by oxidative stress in different cell types. *IUBMB Life* 2000;50:291–9.
26. Chiarugi P, Pani G, Giannoni E, et al. Reactive oxygen species as essential mediators of cell adhesion: the oxidative inhibition of a FAK tyrosine phosphatase is required for cell adhesion. *J Cell Biol* 2003;161:933–44.
27. Begonja AJ, Gambaryan S, Geiger J, et al. Platelet NAD(P)H-oxidase-generated ROS production regulates  $\alpha$ IIb $\beta$ 3-integrin activation independent of the NO/cGMP pathway. *Blood* 2005;106:2757–60.
28. Alexandrova AY, Kopnin PB, Vasiliev JM, Kopnin BP. ROS up-regulation mediates Ras-induced changes of cell morphology and motility. *Exp Cell Res* 2006;312:2066–73.
29. Blaschke F, Stawowy P, Goetze S, et al. Hypoxia activates  $\beta$ 1-integrin via ERK 1/2 and p38 MAP kinase in human vascular smooth muscle cells. *Biochem Biophys Res Commun* 2002;296:890–6.
30. Green CE, Pearson DN, Camphausen RT, Staunton DE, Simon SI. Shear-dependent capping of L-selectin and P-selectin glycoprotein ligand 1 by E-selectin signals activation of high-avidity  $\beta$ 2-integrin on neutrophils. *J Immunol* 2004;172:7780–90.
31. Sato T, Yamochi T, Yamochi T, et al. CD26 regulates p38 mitogen-activated protein kinase-dependent phosphorylation of integrin  $\beta$ 1, adhesion to extracellular matrix, and tumorigenicity of T-anaplastic large cell lymphoma Karpas 299. *Cancer Res* 2005;65:6950–6.
32. Da Silva MS, Siddiqui J, Halverson A, Wilasrusmee C, Bruch D, Kittur DS.  $\beta$ 1-Integrin-ligand disengagement induces *in vitro* capillary tube disruption mediated by p38 MAPK activity. *Surgery* 2003;134:164–8.
33. Hughes PE, Renshaw MW, Pfaff M, et al. Suppression of integrin activation: a novel function of a Ras/Raf-initiated MAP kinase pathway. *Cell* 1997;88:521–30.
34. Chou FL, Hill JM, Hsieh JC, et al. PEA-15 binding to ERK1/2 MAPKs is required for its modulation of integrin activation. *J Biol Chem* 2003;278:52587–97.
35. Wheeler AP, Ridley AJ. Why three Rho proteins? RhoA, RhoB, RhoC, and cell motility. *Exp Cell Res* 2004;301:43–9.
36. Nimmual AS, Taylor LJ, Bar-Sagi D. Redox-dependent downregulation of Rho by Rac. *Nat Cell Biol* 2003;5:236–41.
37. Schwartz MA, Shattil SJ. Signaling networks linking integrins and rho family GTPases. *Trends Biochem Sci* 2000;25:388–91.
38. Giagulli C, Scarpini E, Ottoboni L, et al. RhoA and  $\zeta$  PKC control distinct modalities of LFA-1 activation by chemokines: critical role of LFA-1 affinity triggering in lymphocyte *in vivo* homing. *Immunity* 2004;20:25–35.
39. Hedjazifar S, Jenndahl LE, Shimokawa H, Baeckstrom D. PKB mediates c-erbB2-induced epithelial  $\beta$ 1 integrin conformational inactivation through Rho-independent F-actin rearrangements. *Exp Cell Res* 2005;307:259–75.
40. Zhang JS, Ding J, Tang QM, et al. Synthesis and antitumour activity of novel diterpenequinone salvicine and the analogs. *Bioorg Med Chem Lett* 1999;9:2731–6.
41. Tian F, Zhang X, Tong Y, et al. PE, a new sulfated saponin from sea cucumber, exhibits anti-angiogenic and anti-tumor activities *in vitro* and *in vivo*. *Cancer Biol Ther* 2005;4:874–82.

# Molecular Cancer Research

## Salvicine Inactivates $\beta_1$ Integrin and Inhibits Adhesion of MDA-MB-435 Cells to Fibronectin via Reactive Oxygen Species Signaling

Jin Zhou, Yi Chen, Jing-Yu Lang, et al.

*Mol Cancer Res* 2008;6:194-204.

**Updated version** Access the most recent version of this article at:  
<http://mcr.aacrjournals.org/content/6/2/194>

**Cited articles** This article cites 41 articles, 15 of which you can access for free at:  
<http://mcr.aacrjournals.org/content/6/2/194.full#ref-list-1>

**Citing articles** This article has been cited by 4 HighWire-hosted articles. Access the articles at:  
<http://mcr.aacrjournals.org/content/6/2/194.full#related-urls>

**E-mail alerts** [Sign up to receive free email-alerts](#) related to this article or journal.

**Reprints and Subscriptions** To order reprints of this article or to subscribe to the journal, contact the AACR Publications Department at [pubs@aacr.org](mailto:pubs@aacr.org).

**Permissions** To request permission to re-use all or part of this article, use this link  
<http://mcr.aacrjournals.org/content/6/2/194>.  
Click on "Request Permissions" which will take you to the Copyright Clearance Center's (CCC) Rightslink site.